Linear and Non-linear Transceiver Processing for MIMO-FBMC Systems

Madushanka Soysa
Department of Electrical and Computer Engineering,
University of California at San Diego,
La Jolla, CA
E-mail: msoysa@ucsd.edu

Nandana Rajatheva, and Matti Latva-aho
Department of Communication Engineering,
University of Oulu,
Finland
E-mail: rrajathe@ee.oulu.fi, matti.latva-aho@ee.oulu.fi

***Abstract*—Filter Bank Multicarrier (FBMC) systems has drawn interest as an alternative to orthogonal frequency division multiplexing (OFDM), as FBMC offers higher spectral efficiency and less susceptibility to synchronization errors. One drawback in FBMC systems is the presence of inter-carrier-interference (ICI) and inter-symbol-interference (ISI), which degrades the system performance when operating under fading channels. In this work we consider the bit error rate (BER) performance of a multiple input multiple output (MIMO) FBMC system. We evaluate the performance of linear and non-linear transceiver processing techniques, which attempt to mitigate the effect of ICI and ISI in MIMO FBMC systems. Simulation results are presented to evaluate and compare the transceiver processing techniques discussed.**

***Index Terms* - Filter bank, OQAM, receiver processing, precoding**

I. Introduction

Multicarrier modulation (MCM) techniques are popular in wireless communication systems as they offer robustness against the frequency selectivity of wireless channels. Orthogonal frequency division multiplexing (OFDM) is the most widely used class of MCM currently. However, in OFDM a guard interval or a cyclic prefix is used to eliminate the inter-symbol interference (ISI), which reduces the spectral efficiency. Further, the rectangular pulse shape used in OFDM increases its susceptibility to synchronization errors. As an alternative, filter bank multicarrier (FBMC) was proposed in [1].

In FBMC, the complex data symbol is mapped to real symbols, and the orthogonality between carriers and symbols is then required only in the real axis. This provides flexibility to use a different pulse shape than the rectangular pulse in OFDM, which is better localized in both frequency and time domains [2]. One such prototype filter known as PHYDYAS filter was presented in [3]. In [4], filter designs based on isotropic orthogonal transform algorithm (IOTA) and time-frequency localization (TFL) were investigated. The sensitivity to time asynchronism of PHYDYAS and IOTA filters was studied in [5].

One drawback in FBMC systems is the error floor caused by inter-carrier-interference (ICI) and inter-symbol-interference (ISI). Therefore, receiver processing techniques and precoding techniques to mitigate the effect of ICI and ISI in FBMC systems need to be designed. In [6], a two-step algorithm, equalization with interference cancelation (EIC) was proposed, and evaluated for prototype filters derived through the optimization with respect to the TFL criterion based on IOTA prototype function, in a single antenna FBMC system. Precoding techniques based on the signal-to-leakage-power-and-noise-ratio (SLNR) for MIMO FBMC systems were presented with some assumptions in [7] and [8].

In this work we evaluate the performance of linear receiver processing and precoding techniques in MIMO FBMC systems. We further evaluate the performance of the EIC method proposed in [6], for MIMO FBMC systems. We investigate the performance of an iterative EIC technique, and the performance of EIC in conjunction with error correction coding. We further propose a new iterative precoding technique to minimize the ICI and ISI, and lower the error floor. The performance of these precoding and receiver processing techniques are evaluated using the average bit error rate (BER) as the performance metric through simulations.

The rest of this paper is organized as follows. In Section II the system model is presented. In Section III linear processing methods to remove ICI are discussed, while in Sections IV and V, non-linear receiver processing and precoding techniques are investigated, respectively. Section VI presents the conclusions.

II. System model

We consider a multicarrier MIMO-FBMC system with $2M$ subcarriers, with a single transmitter and a receiver, each equipped with N_A antennas. A simplified block diagram of the transmitter and receiver is given in Fig. 1 and Fig. 2, respectively.

The filter used is $g[k]$ and the filter length is L. We consider a time-invariant Rayleigh fading channel, where the channel delay spread spans Λ sampling intervals. We assume that all antenna paths undergo independent fading. For the receiver processing techniques discussed, we assume the receiver has perfect channel state information (CSI). For the precoding methods discussed, we assume perfect CSI is available at both the transmitter and the receiver.

This work has been performed in the framework of the FP7 project ICT-317669 METIS, which is partly funded by the EU.

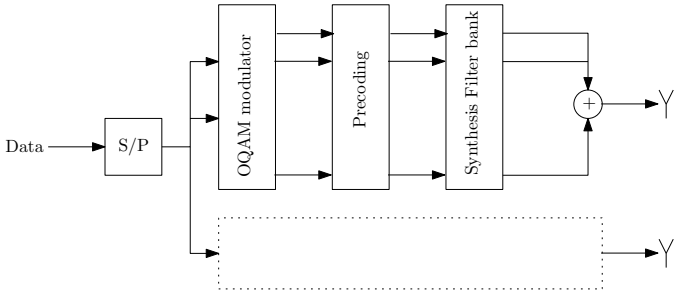

Fig. 1: Transmitter system model

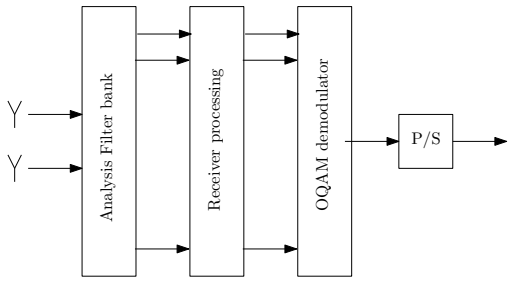

Fig. 2: Receiver system model

We use OQAM modulation, and the baseband equivalent transmitted signal from the p-th transmit antenna, $s_p[k]$.

$$\begin{aligned} s_p[k] &= \sum_{m=0}^{2M-1} \sum_{n\in\mathbb{Z}} a_{m,n}^{(p)} g[k-nM] e^{j\frac{\pi m}{M}(k-\frac{L-1}{2})} e^{j\phi_{m,n}} \\ &= \sum_{m=0}^{2M-1} \sum_{n\in\mathbb{Z}} a_{m,n}^{(p)} g_{m,n}[k] \end{aligned} \tag{1}$$

where $a_{m,n}^{(p)}$ is the real valued transmitted symbol with the average symbol energy E_s, $g_{m,n}[k] = g[k - nM]e^{j\frac{\pi m}{M}(k-\frac{L-1}{2})}e^{j\phi_{m,n}}$ and $\phi_{m,n} = \frac{\pi}{2}(n+m) - \pi nm$ [1]. The received signal by the q-th receiver antenna, $r_q[k]$,

$$r_q[k] = \sum_{p=1}^{N_A} \sum_{l=0}^{\Lambda-1} h_{p,q}[l] s_p[k-l] + w_q[k] \tag{2}$$

where $h_{p,q}[l]$ is the channel fading gain in the l-th tap and $w_q[k]$ is the background noise assumed to be zero-mean Gaussian with variance N_0. We have

$$y_{m',n'}^{(q)} \triangleq \sum_{k\in\mathbb{Z}} r_q[k] g_{m',n'}^*[k] \tag{3}$$

$$\begin{aligned} &= \sum_{p=1}^{N_A} \sum_{m=0}^{2M-1} \sum_{n\in\mathbb{Z}} a_{m,n}^{(p)} e^{j(\phi_{m,n}-\phi_{m',n'}+\pi(m-m')n')} \\ &\times \sum_{l=0}^{\Lambda-1} h_{p,q}[l] e^{-j\frac{\pi ml}{M}} \alpha_g((n'-n)M-l, m-m') \\ &+ \tilde{w}_{m',n'}^{(q)} \end{aligned} \tag{4}$$

where $\alpha_g(x,y) = \sum_{k\in\mathbb{Z}} g[k+x]g[k]e^{j\frac{\pi}{M}(y)(k-\frac{L-1}{2})}$ and $\tilde{w}_{m',n'}^{(q)} = \sum_{k\in\mathbb{Z}} w_q[k] g_{m',n'}^*[k]$.

Using matrix notation to represent the signal from all receiver antennas, we have,

$$\begin{aligned} Y_{m',n'} &= \sum_{m=0}^{2M-1} \sum_{n\in\mathbb{Z}} e^{j(\phi_{m,n}-\phi_{m',n'}+\pi(m-m')n')} \sum_{l=0}^{\Lambda-1} e^{-j\frac{\pi ml}{M}} \\ &\times \alpha_g((n'-n)M-l, m-m') H[l] A_{m,n} + W_{m',n'} \\ &= \sum_{m=0}^{2M-1} \sum_{n\in\mathbb{Z}} e^{j(\frac{\pi}{2}(m-m'+n-n')-\pi(n-n')m)} \sum_{l=0}^{\Lambda-1} e^{-j\frac{\pi ml}{M}} \\ &\times \alpha_g((n'-n)M-l, m-m') H[l] A_{m,n} + W_{m',n'} \end{aligned} \tag{5}$$

where $Y_{m',n'}$, $A_{m,n} = [a_{m,n}^{(p)}]$ and $W_{m',n'} = [\tilde{w}_{m',n'}^{(q)}]$ are length N_A vectors, and $H[l] = [h_{p,q}[l]]$ is a $N_A \times N_A$ matrix.

We can rewrite $Y_{m',n'}$ as follows,

$$Y_{m',n'} = \sum_{m=0}^{2M-1} \sum_{n\in\mathbb{Z}} H_{m,m-m',n'-n} A_{m,n} + W_{m',n'} \tag{6}$$

where $H_{m,n,m',n'} = e^{j(\frac{\pi}{2}(m-m'+n-n')-\pi(n-n')m)} \sum_{l=0}^{\Lambda-1} H[l] \times \alpha_g((n'-n)M-l, m-m')e^{-j\frac{\pi ml}{M}}$.

Zero forcing (ZF) is used at the receiver, to remove the antenna interference from the output of the synthesis filterbank.

$$\begin{aligned} \tilde{Y}_{m',n'} &= \Re\left\{ H_{m',0,0}^{-1} Y_{m',n'} \right\} \\ &= A_{m',n'} + \Re\Big\{ \sum_{(m,n)\neq(m',n')} H_{m',0,0}^{-1} H_{m,m-m',n'-n} \\ &\times A_{m,n} \Big\} + \Re\left\{ H_{m',0,0}^{-1} W_{m',n'} \right\} \end{aligned} \tag{7}$$

The interference component $I_{m',n'}$ is given by

$$I_{m',n'} = \Re\left\{ \sum_{(m,n)\in V_{m',n'}} H_{m',0,0}^{-1} H_{m,m-m',n'-n} A_{m,n} \right\} \tag{8}$$

where the neighborhood of (m',n'), $V_{m',n'} \triangleq \{(m,n) | m,n \in \mathbb{Z}, 0 \le m \le 2M-1, \sum_{l=0}^{\Lambda-1} |\alpha_g((n'-n)M-l, m-m')| > 0, (m,n) \neq (m',n')\}$.

A. ISI and ICI

In this paper, we use the term ICI to refer to the interference to the symbol of interest from symbols in other subcarriers in the same time index. The term ISI is used to refer to the interference from symbols in different time indices in all subcarriers. The ISI and ICI depends on the pulse shape, channel and the data. Table I shows the values of $\alpha_g((n'-n)M-l, m-m')$, for a few values of the parameters $m-m'$, $n-n'$ and l, for the PHYDYAS filter $g[k]$.

Investigating the behavior of $\alpha_g((n'-n)M-l, m-m')$, we note that a significant portion of ICI occurs from the adjacent subcarriers. Depending on the delay spread of the channel, ISI may occur from symbols transmitted up to 7 indices both prior to, and after from the symbol of interest. Because of that, as we are not using a cyclic prefix, we are unable to process the received signal as a block to remove ISI through linear equalization techniques.

$(n'-n,l)$	(0,0)	(0,1)	(0,2)	(1,0)	(1,1)	(1,2)
$m-m'=0$	1	0.9917	0.9672	0.5644j	0.6509j	0.7330j
$m-m'=1$	0.2393j	0.2341j-0.0466	0.2190j-0.0907	0.2058j	0.0426+0.2092j	0.0842+0.2033j
$m-m'=2$	0	0	0	0	0	0

TABLE I: PHYDYAS filter $\alpha_g((n'-n)M-l, m-m')$

III. Linear processing methods to remove ICI

In this section we look at the performance of linear processing techniques which we can design to remove the ICI. From (6), we can rewrite the received signal as follows,

$$Y_{n'} = \sum_{n\in\mathbb{Z}} H_{n'-n}A_n + W_{n'} \tag{9}$$

where Y_n is the vector of the received signals over all subcarriers and antennas, A_n is the vector of symbols transmitted over all subcarriers in the n-th symbol time and

$$H_{n'-n} = \begin{pmatrix} H_{0,0,n'-n} & \cdots & H_{2M-1,2M-1,n'-n} \\ H_{0,-1,n'-n} & \cdots & H_{2M-1,2M-2,n'-n} \\ \vdots & \ddots & \vdots \\ H_{0,-2M+1,n'-n} & \cdots & H_{2M-1,0,n'-n} \end{pmatrix}. \tag{10}$$

We can use a precoding matrix (G_n) and a receiver processing matrix (F_n) to represent the linear processing done at the transmitter and the receiver in the n-th time index. The received signal $Y_{n'}$ from (9) will be modified as follows.

$$Y_{n'} = \sum_{n\in\mathbb{Z}} H_{n'-n}G_nA_n + W_{n'} \tag{11}$$

The symbol estimate after receiver processing is given by

$$\begin{aligned}\hat{A}_{n'} &= \mathbb{D}\ [\Re\{F_{n'}Y_{n'}\}] \\ &= \mathbb{D}\left[\Re\left\{F_{n'}\left(\sum_{n\in\mathbb{Z}} H_{n'-n}G_nA_n + W_{n'}\right)\right\}\right]\end{aligned} \tag{12}$$

where $\mathbb{D}[\cdot]$ denotes minimum distance hard decision mapping to a symbol from the alphabet and $\Re\{\cdot\}$ represents the real part of the complex argument.

Define the block diagonal matrix

$$H_{\text{diag}} = \begin{pmatrix} H_{0,0,0} & & 0 \\ & \ddots & \\ 0 & & H_{2M-1,0,0} \end{pmatrix}. \tag{13}$$

- Linear pre-equalization at transmitter: To remove the ICI while keeping the transmitter symbols real valued, the precoding matrix derived is $G_n = \Re\{H_{\text{diag}}^{-1}H_0\}^{-1}$ and the receiver processing matrix is $F_n = H_{\text{diag}}^{-1}$. Here H_{diag}^{-1} resembles to the removal of antenna interference in each subcarrier separately while $\Re\{H_{\text{diag}}^{-1}H_0\}^{-1}$ removes the remaining ICI.
- Linear equalization at receiver: To remove ICI at the receiver, $G_n = I$ and $F_n = \Re\{H_{\text{diag}}^{-1}H_0\}^{-1}H_{\text{diag}}^{-1}$.

Simulation results

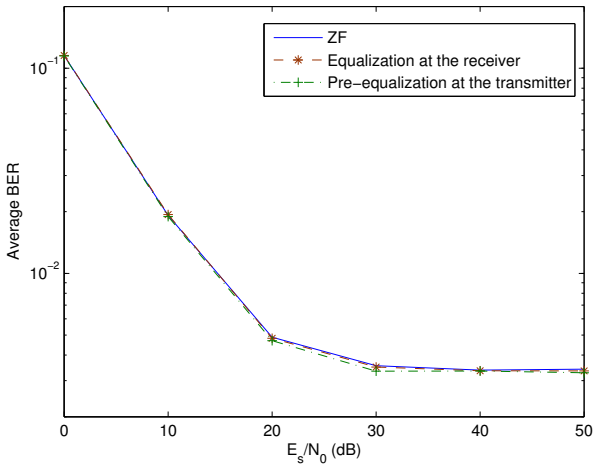

Fig. 3: Average BER with linear processing ($\Lambda = 2$, $2M = 16$, $L = 63$, $N_A = 2$, $\mathbb{E}\left[|h_{p,q}[1]|^2\right] = 0.5$)

For the simulations in this section and the proceeding sections, we consider a MIMO system with 2 transmitter and receiver antennas ($N_A = N_A = 2$) and the number of subcarriers ($2M$) is chosen to be 16. We assume that the channel between p-th transmitter antenna and the q-th receiver antenna is a two-path time-invariant Rayleigh channel. The average gain of the first path is assumed to be unity; i.e. $\mathbb{E}\left[h_{p,q}[0]h_{p,q}^*[0]\right] = 1$.

Average bit error rate (BER) with linear equalization and pre-equalization of the system is shown in Fig. 3. We have plotted the average BER with only the removal of antenna interference by ZF as shown in Eq. (7) for comparison. As we can see, the linear processing techniques derived here do not improve the BER performance by a noticeable margin. Even though the ICI is removed, the linear processing fails to remove the ISI and may even enhance the ISI, which makes linear processing techniques ineffective.

IV. Non-linear processing methods to remove ISI/ICI at the receiver

A. EIC receiver processing

In this section we look at the performance of equalization with interference cancellation (EIC) method proposed in [9], in a MIMO FBMC system with PHYDYAS filter. Here we first detect the received symbols using zero-forcing. From (6), we have

$$\hat{A}_{m,n}^{(1)} = \mathbb{D}\left[\Re\{H_{m',0,0}^{-1}Y_{m',n'}\}\right] \tag{14}$$

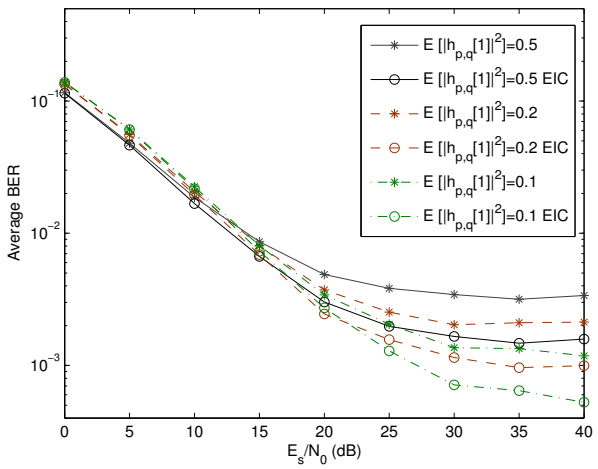

Fig. 4: Average BER with EIC ($\Lambda = 2$, $2M = 16$, $L = 63$, $N_A = 2$)

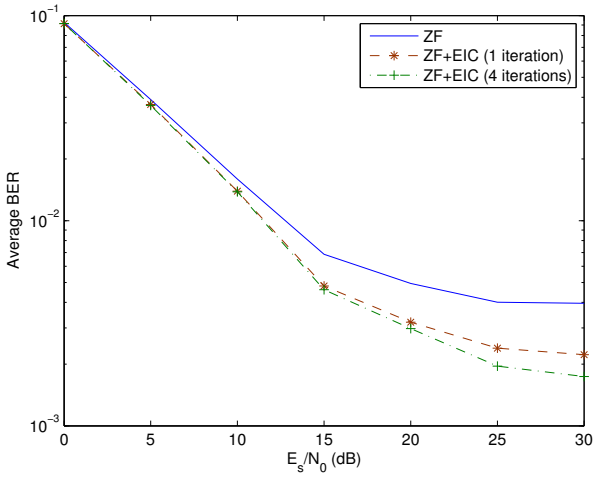

Fig. 5: Average BER with EIC ($\Lambda = 2$, $2M = 16$, $L = 63$, $N_A = 2$, $\mathbb{E}\left[|h_{p,q}[1]|^2\right] = 0.5$)

Then, we use these estimated symbol values ($\hat{A}^{(1)}_{m,n}$) to calculate the ICI and ISI, and remove it from the received signal. Then we again perform zero forcing to obtain a new estimate of the received symbols.

$$\hat{A}^{(2)}_{m,n} = \mathbb{D}\left[\Re\Big\{H^{-1}_{m',0,0}\big(Y_{m',n'} - \sum_{(m,n)\in V_{m',n'}} H_{m,m-m',n'-n}\hat{A}^{(1)}_{m,n}\big)\Big\}\right] \quad (15)$$

We can iterate this process to improve the symbol estimation, at the expense of increased computational complexity and memory. For each additional iteration, we require $N_A N_A |V_{m',n'}|$ additional multiplications to estimate the interference $\sum_{(m,n)\in V_{m',n'}} H_{m,m-m',n'-n}\hat{A}^{(\cdot)}_{m,n}$. Further, if the maximum time index difference of elements in $V_{m',n'}$ is Δn for all (m', n'), the r-th iteration to estimate $\hat{A}^{(r)}_{m',n'}$ requires knowledge of a subset of symbols in the interval $[n' - \frac{\Delta n}{2}r, n' + \frac{\Delta n}{2}r]$. Hence, the amount of memory required increases linearly with the number of iterations. However, the main performance challenge here is the error propagation. If the initial symbol decision has a lot of errors, the subsequent EIC process is unable to remove the interference.

Simulation results

The average gain of the first path is assumed to be unity; i.e. $\mathbb{E}\left[|h_{p,q}[0]|^2\right] = 1$. Fig. 4 shows the average BER parameterized by the average gain of the second path $\mathbb{E}\left[|h_{p,q}[1]|^2\right]$.

The performance may be improved with additional iterations, as can be seen from Fig. 5, where we have taken $\mathbb{E}\left[|h_{p,q}[1]|^2\right] = 0.5$.

B. Error correction coding

Forward error correction (FEC) can be used in an attempt to remove the error floor by improving the accuracy of the initial symbol estimation $\hat{A}^{(1)}_{m,n}$. Here we make use of convolutional codes. Fig. 6 shows the basic receiver model.

Simulation results

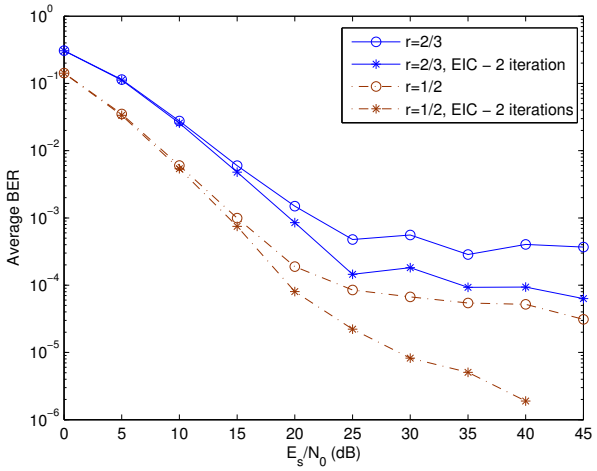

Fig. 7: Average BER with EIC and FEC ($\Lambda = 2$, $2M = 16$, $L = 63$, $N_A = 2$, $\mathbb{E}\left[|h_{p,q}[1]|^2\right] = 0.2$)

Fig. 7 shows the average BER when convolutional code based FEC is used in conjunction with EIC. We have evaluated performance with two different convolution codes of rates $\frac{2}{3}$ and $\frac{1}{2}$, and memory 3. For comparison, average BER without EIC is also presented. We note that the error floor can be driven down to $10^{-5} - 10^{-6}$ region with the use of the rate $\frac{1}{2}$ convolutional code and EIC.

V. Non-linear processing at the transmitter

A. Tomlinson Harashima precoding (THP)

At the transmitter, the expected interference due to ICI and ISI is calculated using (8). We then update the transmitted symbols to cancel the possible expected interference [10].

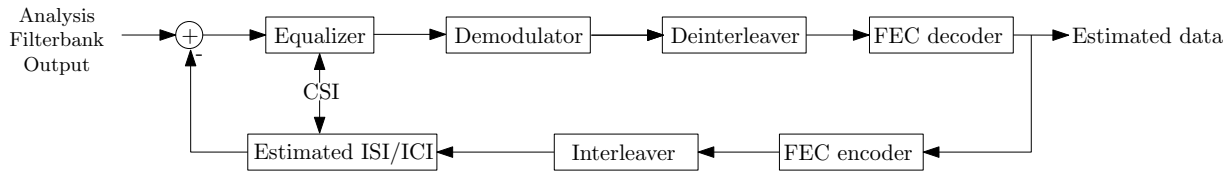

Fig. 6: Receiver system model incorporating FEC with EIC

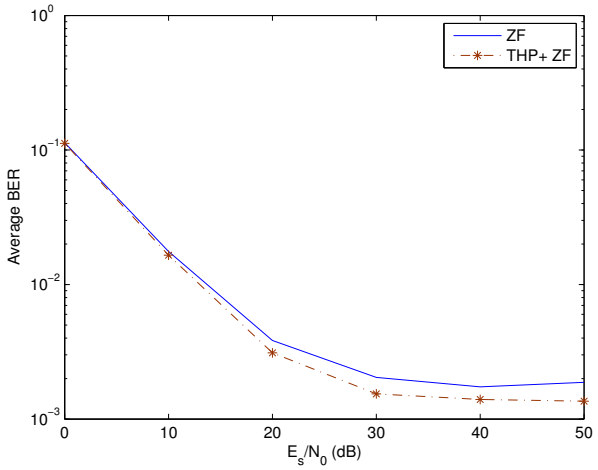

Fig. 8: Average BER with THP ($\Lambda = 2$, $2M = 16$, $L = 63$, $N_A = 1$, $\mathbb{E}\left[|h_{p,q}[1]|^2\right] = 0.5$)

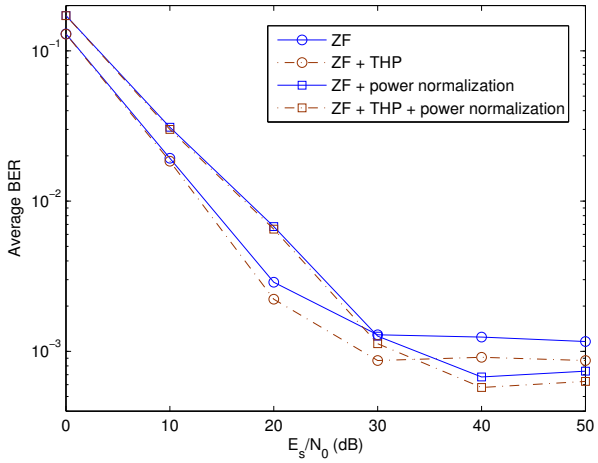

Fig. 9: Average BER with THP precoding and power normalization ($\Lambda = 2$, $2M = 16$, $L = 63$, $N_A = 1$, $\mathbb{E}\left[|h_{p,q}[1]|^2\right] = 0.2$)

Hence, the transmitted symbols can be written as

$$\overline{A}^{(1)}_{m',n'} = A_{m',n'} - \Re\Big\{ \sum_{(m,n)\in V_{m',n'}} H^{-1}_{m',0,0} H_{m,m-m',n'-n} A_{m,n} \Big\}. \tag{16}$$

However, since the interference occurs from symbols transmitted both prior to and after from each symbol, the updating of the symbol in position (m', n') affects its interference to symbols transmitted prior to it. Hence, the technique in (16) cannot completely remove the interference. We can further iterate this process to improve the interference cancellation, incurring higher computational complexity and memory requirements, similar to EIC in section IV-A.

$$\overline{A}^{(r+1)}_{m',n'} = A^{(r)}_{m',n'} - \Re\Big\{ \sum_{(m,n)\in V_{m',n'}} H^{-1}_{m',0,0} H_{m,m-m',n'-n} A^{(r)}_{m,n} \Big\} \tag{17}$$

To avoid the possible unbounded transmitter power increase due to precoding using (16), the usual practice is to use the modulo operation to keep $\overline{A}^{(1)}_{m',n'}$ within the boundaries of the original alphabet.

Simulation results

The average BER of the MIMO FBMC system with THP precoding to cancel the interference is presented in Fig. 8. The performance without precoding is plotted for comparison.

We note that the precoding technique in (16) has reduced the error floor in the MIMO FBMC system. However, this does not offer significant performance improvement over ZF. This is because the precoding technique in (16) cannot completely remove the interference, as discussed earlier.

B. THP with power normalization

Through the observation of error patterns, we note that the main cause of errors are due to subcarriers with weak channels, adjacent to subcarriers with strong channels. In this case, the interference from adjacent subcarriers is too large relative to the source signal in that subcarrier for accurate detection of the symbols. Hence, we look at power normalization to improve the performance. Here we would multiply the source symbols before transmission with an amplification factor, so that the average energy of source symbols in each subcarrier is maintained to be equal.

Simulation results

The average BER with the power normalization is given in Fig. 9, in which the average BER without power normalization is also plotted for comparison. The average BER in the $E_s/N_0 < 30$dB region has worsened with power normalization. This could be because the power normalization may worsen the average signal-to-noise-ratio at the receiver depending on the channel, and noise is a more significant cause of errors in low E_s/N_0 region than interference. However, we can see that the power normalization has lowered the error floor. Yet, power normalization with THP precoding offers only marginal performance improvements.

C. Punctured THP

In this section we look at the error performance of the MIMO FBMC system with THP precoding, representing the symbol positions by vertices of a graph and the interference between symbols with weighted edges of the graph.

Define a weighted digraph $G_I \triangleq (V_I, E_I)$, where the set of vertices

$$V_I = \{(m,n) | m,n \in \mathbb{Z}, 0 \leq m \leq 2M-1\} \tag{18}$$

and the set of directed edges

$$E_I = \{((m,n),(m',n')) | (m,n),(m',n') \in V_I, (m,n) \in V_{m',n'}\} \tag{19}$$

The weight function $f_I : E_I \to \mathbb{R}$ is defined as

$$f_I((m,n),(m',n')) = ||\Re\{H^{-1}_{m',0,0} H_{m,m-m',n'-n}\}||_F. \tag{20}$$

The iterative approach in (17) would converge and can be used to remove the interference between symbols if the sum of weights in cycles with any one common vertex in the interference graph G_I is less than unity. One solution to improve the performance of precoding technique is to attempt to remove the cycles in the interference graph with high gains. If this is done, we can iterate the THP algorithm to completely remove the interference. Hence, we look at removing a symbol position which contributes to cycles with large gains in the interference graph. We call this punctured THP. Note that the gains in the interference graph depends only on the channel. If we assume perfect CSI both at the transmitter and the receiver, the transmitter and the receiver will be able to make these calculations independently.

Calculating gains of all the cycles in the interference graph will result in computational complexity. Therefore, we propose a suboptimal alternative parameter $\tau_{(m',n')}$,

$$\tau_{(m',n')} = \sum_{(m,n) \in V_{m',n'}} f_I((m,n),(m',n')) \tag{21}$$

to be used as the condition of removal of symbol positions. Here, a subset of symbols at positions with the sum of weights of the incoming paths ($\tau_{(m',n')}$) greater than a predetermined threshold would be removed. In a time varying channel, this calculation would need to be done for all symbols. In the time-invariant channel we consider, once is sufficient for each subcarrier, as it would remain the same, along time. Here the aim is to improve the error floor, at a loss of average throughput.

Simulation results

The performance of the punctured THP algorithm, where we remove every third symbol position which has the sum of path gains $\tau_{(m',n')} > 2$, is presented in Fig. 10. We have plotted the average BER curves of the punctured transmission scheme with and without THP, and the average BER without puncturing for comparison. We see that the error floor has reduced due to puncturing. Further, the use of THP with puncturing has lowered the error floor by approximately 60 times, and the throughput loss incurred due to puncturing in the simulation was found to be only 0.67%.

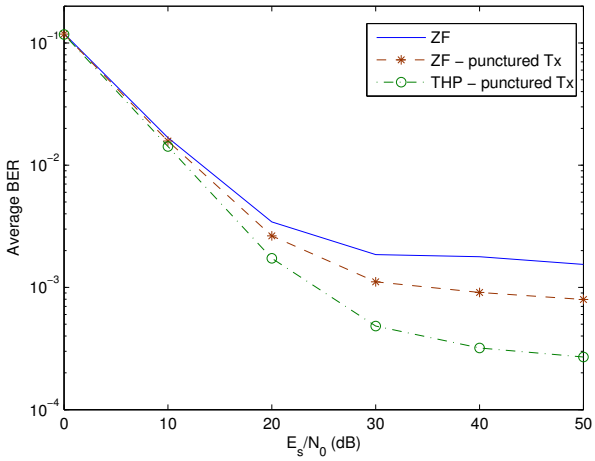

Fig. 10: Average BER with punctured THP ($\Lambda = 2$, $2M = 16$, $L = 63$, $N_A = 2$, $\mathbb{E}\left[|h_{p,q}[1]|^2\right] = 0.5$, $\tau_{(m',n')} = 2$)

VI. Conclusion

In this paper we evaluated the performance of linear and non-linear transceiver processing techniques to improve the average BER of MIMO FBMC systems. The linear processing techniques did not offer any system improvements. The non-linear receiver processing technique, EIC, when used in conjunction with forward error correction, can eliminate the error floor of the system. THP based iterative precoding algorithm, punctured THP, can significantly lower the system error floor.

References

[1] P. Siohan, C. Siclet, and N. Lacaille, "Analysis and design of ofdm/oqam systems based on filterbank theory," *IEEE Transactions on Signal Processing*, vol. 50, no. 5, pp. 1170–1183, 2002.

[2] B. Farhang-Boroujeny, "Ofdm versus filter bank multicarrier," *IEEE Signal Processing Magazine*, vol. 28, no. 3, pp. 92–112, 2011.

[3] M. Bellanger, "Specification and design of a prototype filter for filter bank based multicarrier transmission," in *IEEE International Conference on Acoustics, Speech, and Signal Processing, 2001. Proceedings. (ICASSP '01). 2001*, vol. 4, 2001, pp. 2417–2420 vol.4.

[4] P. Siohan and C. Roche, "Cosine-modulated filterbanks based on extended gaussian functions," *IEEE Transactions on Signal Processing*, vol. 48, no. 11, pp. 3052–3061, 2000.

[5] Y. Medjahdi, D. Le Ruyet, D. Roviras, H. Shaiek, and R. Zakaria, "On the impact of the prototype filter on fbmc sensitivity to time asynchronism," in *2012 International Symposium on Wireless Communication Systems (ISWCS)*, 2012, pp. 939–943.

[6] H. Lin, C. Lele, and P. Siohan, "Equalization with interference cancellation for hermitian symmetric ofdm/oqam systems," in *IEEE International Symposium on Power Line Communications and Its Applications, 2008. ISPLC 2008.*, 2008, pp. 363–368.

[7] U. Jayasinghe, N. Rajatheva, and M. Latva-aho, "Application of a leakage based precoding scheme to mitigate intrinsic interference in fbmc," in *IEEE International Conference on Communication*, June 2013.

[8] ——, "Leakage based multi user beamforming scheme to mitigate interference in mimo-fbmc," in *WSA 2013 - 17th International ITG Workshop on Smart Antennas*, March 2013.

[9] H. Lin and P. Siohan, "A new transceiver system for the ofdm/oqam modulation with cyclic prefix," in *IEEE 19th International Symposium on Personal, Indoor and Mobile Radio Communications, 2008*, 2008.

[10] C. Windpassinger, R. F. H. Fischer, T. Vencel, and J. Huber, "Precoding in multiantenna and multiuser communications," *IEEE Transactions on Wireless Communications*, vol. 3, no. 4, pp. 1305–1316, 2004.